ELSEVIER

Journal of Electron Spectroscopy and Related Phenomena 121 (2001) 265–279

JOURNAL OF ELECTRON SPECTROSCOPY and Related Phenomena

www.elsevier.com/locate/elspec

Importance of structural order for the low surface energy of perfluoroalkyl substituted polymethacrylates

J. Lüning[a,*], D.Y. Yoon[b], J. Stöhr[a]

[a]*Stanford Synchrotron Radiation Laboratory, MS 69, P.O. Box 20450, Stanford, CA 94209, USA*
[b]*School of Chemistry, Seoul National University, Seoul 151-747, South Korea*

Received 28 February 2001; received in revised form 14 April 2001; accepted 20 April 2001

Abstract

Low surface energy coatings or anti-wetting agents play an essential role in microelectronics, anti-fogging and anti-fouling applications, and even have promising medical applications. Currently, perfluoroalkyl substituted polymethacrylates (PFPMs) are widely in use, and the anti-wetting properties of these and related polymers are believed to arise from the segregation of CF_3 groups to the surface. However, proof of a direct correlation between surface energies and surface structure, and the importance of the order in the underlying bulk is still lacking. Here we report near edge X-ray absorption fine structure (NEXAFS) results which establish such a correlation. Our studies of three PFPMs with, respectively, isotropic, nematic, and smectic A bulk phases at room temperature reveal in all cases a greater order at the surface than in the bulk. The surface order parameter is found to correlate with the surface energy, which we find indeed to be lowered by segregation of CF_3 groups to the film surface. Most importantly, temperature dependent NEXAFS measurements in the 20–140 °C range, covering bulk phase transitions from smectic A to nematic to isotropic, show that it is the bulk order (phase) which ultimately limits the achievable surface order, and hence the surface properties.

Keywords: Low surface energy coatings; Perfluoroalkyl substituted polymethacrylates

1. Introduction

Polymers have an increasing number and diversity of applications [1], which is driven by the growing ability to tailor polymer properties to the specific needs of an application. An important class of applications are polymer coatings that may have thicknesses of only a few nanometers. Lubrication, separation and protection are among the main purposes of such coatings. With the increasing demand in the quality of such coatings grows the need for experimental tools, which are capable to investigate those properties. Traditional techniques like neutron scattering and optical spectroscopy, the techniques of choice for the study of bulk properties, typically lack the sensitivity and selectivity to address the properties of a thin polymer film or its surface. Photoemission spectroscopy and, in particular, X-ray photoemission spectroscopy [2], which is discussed in several articles of this issue, is a powerful tool to study polymer surfaces. However, as an electron-

*Corresponding author.
E-mail address: luning@stanford.edu (J. Lüning).

0368-2048/01/$ – see front matter
PII: S0368-2048(01)00339-5

based technique, it probes only the outermost surface region due to the short mean free path of electrons in matter[1]. Additional limitations for the investigation of polymers originate from sample charging and the requirement to perform these experiments in an (ultra)-high vacuum environment.

In this article we will show that soft X-ray absorption spectroscopy, in particular, the analysis of the near edge X-ray absorption fine structure (NEXAFS) and its polarization dependence [3], offers unique capabilities for the investigation of thin polymer films. NEXAFS spectroscopy is particularly powerful when information is sought on the composition and bond orientation in thin films or near the surface of bulk polymers.

Low surface energy polymers form an important class of thin film coatings. Such coatings are widely used for a broad variety of 'anti'-applications like anti-wetting, anti-fogging or anti-fouling. They are important for microelectronics, textile, optical and even medical applications [4]. Such polymer coatings have surface energies that are much lower than those of 'traditional' solids. Metals, for example, have surface energies of up to 1000 dyn/cm, and even larger values can be found for covalent materials like diamond. Low surface energy polymers, on the other hand, can have values below 20 dyn/cm [5,6]. This is lower than the surface tension of water (70 dyn/cm at 20 °C) and even oil (of the order of 30 dyn/cm at 20 °C). Thus, even if oil were spilled on a low surface energy polymer film, it would not spread out to cover the surface, but the oil would form droplets instead, which could easily be removed.

In general, polymers have low surface energies due to the weak interaction between the different molecular groups of the polymer chain [7]. Hence, the groups forming the polymer surface do not lack a significant interaction on their exposed surface side and the gain in surface energy from adding neighbors to these surface groups is small. In semifluorinated polymers, the surface energy is further lowered by reducing the polarizability of the groups that form the polymer surface. This reduces the van der Waals interaction, which generally dominates the interaction at a liquid–vapor interface.

Perfluoroalkyl substituted polymethacrylates (PFPMs) have emerged as the most widely used low surface energy polymer coatings. In these polymers, fluorocarbon chains are attached to the carboxyl group of the polymethylmethacrylate (PMMA) side chains, resulting in a polymer structure of the form

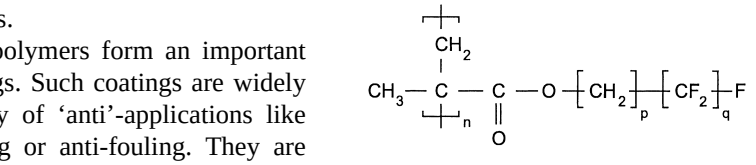

The anti-wetting properties of these and related polymers are believed to arise from the segregation of CF_3 groups to the surface [5,8–10], which have a low polarizability due to the strongly ionic character of their molecular bonds.

From optical spectroscopy and neutron/X-ray scattering it is known that the bulk of semifluorinated polymers can have different ordered phases [5,11,12]. Crystalline, smectic, and nematic ordered phases [13] as well as isotropic disordered phases can be found, depending on the length of the side chains, their number of CF_2 units and the temperature. On the other hand, little is known about the surface of these polymers. Yet it is clear that the low surface energy properties are determined by the topmost surface region alone. The missing correlation between surface and bulk structure has so far hampered the understanding of the relationship between bulk properties and surface energy [5,14]. Hence, improvements of low surface energy coatings have been mostly accomplished by trial and error.

In this article, we report how NEXAFS spectroscopy can be used to establish the missing link between surface and bulk order. We will show that although the surface energy is indeed determined by segregation of CF_3 groups to the film surface, it is the bulk order of the film that ultimately limits the lowering of the surface energy.

We have investigated three very similar PFPM

[1]The sampling depth of XPS can also be altered by varying the photon incidence and/or electron take-off angle [see e.g. G. Beamson et al., J. Mater. Chem. 7 (1997) 75]. The absorption yield technique presented here, however, can sample deeper into the material. In addition, absorption spectroscopy allows in most cases a better distinction of different sample components, because of the generally richer fine structure of absorption spectra in comparison with XPS spectra.

polymers, which all have fluorocarbon side chains of the type $(CH_2)_p(CF_2)_qF$ attached to the carboxyl group of the PMMA side chains. At room temperature these polymer films have different bulk phases and they show a series of matching phase transitions. The bulk of the polymer with the longest side chains, $F8=(CH_2)_2(CF_2)_8F$, exhibits a smectic A phase at room temperature. This phase is the highest degree of bulk order found among the three investigated polymers. A phase transition to a nematic bulk phase is observed around 80 °C, and around 120 °C a second phase transition to a disordered isotropic bulk phase occurs. The hydrocarbon backbone itself does not have any preferential orientation in any of the bulk phases (nor in the case of the other two films), but it runs randomly through the film.

Reducing the length of the side chains by one CF_2 group gives the polymer $F7=(CH_2)(CF_2)_7F$, whose bulk structure exhibits a nematic ordered phase at room temperature. This nematic order is lost around 80 °C, where a phase transition to an isotropic bulk phase occurs. The third polymer $F6=(CH_2)_2(CF_2)_6F$ has no ordered bulk phase in the studied temperature range, i.e. the side chains have an isotropic, random orientation like the backbone.

With decreasing length of the side chains we determine the surface energy to increase from 8 dyn/cm for F8, to 9 dyn/cm for F7, and 10 dyn/cm for F6. This indicates that chemical composition or bulk concentration of CF_3 groups cannot alone be responsible for the surface energy lowering since the relative amount of CF_3 groups is the highest for F6 and the lowest for F8. Instead, this observation points to a relation between bulk order and surface energy, which is explored in the present paper.

2. Experimental

The fluorocarbon polymers have been prepared by atom transfer radical polymerization (ATRP) of the monomers. The monomers were obtained from an esterification reaction of methacryloyl chloride with corresponding alcohols in order to obtain high-molecular-weight samples with a relatively narrow molecular weight distribution [15]. The polymers were soluble in hexafluorobenzene and purified by reprecipitation in chloroform and methanol. The intrinsic viscosities of the polymers in hexafluorobenzene were found to be high, ~1.5 dL/g at 30 °C, indicating high-molecular-weight characteristics (>100 000). Thin polymer films were deposited on silicon wafers by spin-coating using hexafluorobenzene as solvent. We observed no dependence of our results on film thickness in the studied range of some ten nanometers to a few microns.

The surface energy of the three polymer films has been determined with the Zisman plot method from the measured contact angles for several liquids [16]. For the F8 and F7 polymer film, the contact angles remained constant over time, but due to partial solubility of the polymer F6, contact angles for this film had to be measured immediately. An accuracy better than ±0.02 dyn/cm is indicated by the Zisman plots, which is significantly better than the observed decrease in surface energy with increasing number of CF_2 groups in the side chains. The bulk phase behavior of the three polymer films has been determined in the temperature range of 20–140 °C by X-ray diffraction experiments and hot-stage polarized optical microscopy studies of miscibility behavior with perfluoroalkylethers, which are completely miscible at the ambient. The observed bulk order phase transitions are found to be reversible.

High-resolution C K-edge (1s) absorption spectra of the three polymers were measured at the wiggler beamline 10-1 of the Stanford Synchrotron Radiation Laboratory with a photon energy resolution of about 80 meV around the C K absorption edge. The X-rays are elliptically polarized, with 80% horizontal linear and 20% vertical linear polarization in the energy range around 300 eV [17]. All spectra were normalized to the incident photon flux by use of a gold grid reference monitor and, by normalization to a common edge jump in the 330–340 eV region, the plotted spectra correspond to an intensity per C atom [3]. The energy scale was calibrated using the carbon induced structure at 284.7 eV in the monochromator transmission function [3].

Absorption spectra with different surface sensitivity may be recorded simultaneously by means of Auger (AEY) and total electron yield (TEY) detection. In a conventional transmission X-ray absorption experiment one measures the photon absorption coefficient directly, i.e. the photon absorption probability due to excitation of a core electron vacancy. In a yield measurement, on the other hand, the occurrence of an absorption event is detected by

monitoring secondary particles, which are emitted in the decay of the excited core hole. Auger decay is the dominant core hole decay mechanism in the soft X-ray energy region (roughly defined as from 30 eV to 2000 eV) with the fluorescence decay probability increasing with decay energy [18].

AEY measurements monitor the intensity of elastically emitted Auger electrons by means of an electron energy analyzer [3]. The sampling depth is given by the short elastic mean free path of the Auger electrons in the material [19]. Hence, AEY measurements sample only the near subsurface region. In TEY measurements, on the other hand, all electrons emitted from the sample surface are counted, the elastically scattered Auger and all other electrons. The TEY signal is dominated by the low energy electrons excited in the inelastic scattering cascade of the primary Auger electrons. Since the low kinetic energy electrons have undergone several scattering events, TEY probes deeper below the sample surface than AEY.

Around the carbon K-edge the $1/e$ sampling depths of AEY and TEY in polymers are about 1 nm and 10 nm from the free surface [20], respectively. In other words, the top 1 nm (10 nm) gives rise to 67% of the spectral weight in an AEY (TEY) spectrum.

It is well known [3] that electron yield measurements may have inherent problems like saturation effects [21] and sample charging. In case of thin film samples, however, saturation and charging effects are sufficiently suppressed. For film thicknesses below about 100 nm and low incident X-ray intensities charging effects are negligible even for strongly insulating samples like the PFPM polymer films investigated here. Indeed, no charging effects are observed for submicron thin PFPM films.

The TEY spectra were recorded by measuring the sample drain current with a picoampere meter, and a cylindric mirror analyzer (CMA) was used to record the AEY spectra. The CMA energy window was centered on the C KLL Auger peak around 260 eV. The throughput of the analyzer was increased by using a large pass energy of 1000 eV, corresponding to an energy window width of about 16 eV, to obtain a sufficient signal at the diminished photon flux required to avoid radiation damage, as discussed below.

The polarization dependence of the absorption spectra were investigated by changing the orientation of the sample relative to the direction of the elliptically polarized X-rays [17], which major electric field vector component $\vec{E}$ is oriented horizontally. This major $\vec{E}$ component is parallel to the sample surface in the normal incidence geometry ($\Theta = 90°$). By rotating the sample about its vertical axis to a grazing incidence geometry ($\Theta = 20°$), the major $\vec{E}$ component is oriented 20° off the surface normal.

As emphasized and discussed in detail below, fluorocarbon polymers are extremely sensitive to radiation damage. By reducing the incident flux density to about 3×10^9 photons/s spread out over a 2×2 mm^2 area on the sample, we were able to greatly reduce radiation damage. Under these conditions no significant sample damage was observed over the 10-min time period needed for the acquisition of an absorption spectrum. A new beam spot on the sample was selected for each spectrum.

3. Results and discussion

3.1. Chemical composition

Within the single electron approximation of the X-ray absorption process the incident photon is absorbed by exciting a core electron into an unoccupied valence state. In a polymer one probes the atom specific projection of the valence orbitals and the corresponding transitions give rise to sharp resonances in the absorption spectrum [3,22]. The largest and narrowest resonances are observed near the absorption threshold and typically correspond to $1s\rightarrow\pi^*$ transitions with broader $1s\rightarrow\sigma^*$ resonances at higher energies.

Both kinds of signatures can be found in the C K-edge absorption spectrum of PMMA, which is shown by the dash-dotted line in Fig. 1. The dominant peak just above 288 eV corresponds to excitation of C 1s core electrons into the unoccupied π^*-orbital of the C=O bond in the carboxyl group of the PMMA side chains [23]. The shoulder preceding this peak results from excitation into the C–H orbitals. The nearly structureless shape of the absorption spectrum at photon energies above these two resonances is mainly due to excitations into σ^*-orbitals of the C–C bonds in the polymer backbone.

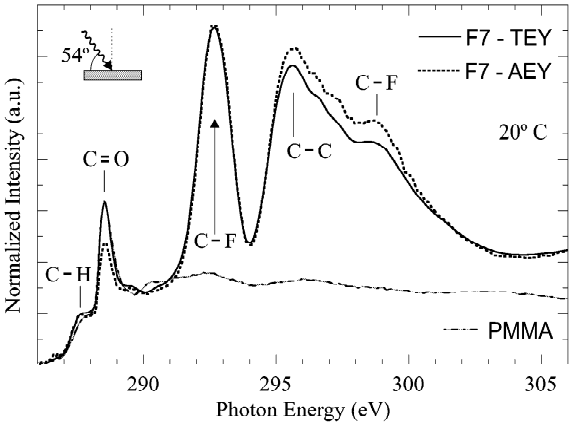

Fig. 1. C K-edge (1s) NEXAFS spectra of PMMA (dashed-dotted) and a thin PFPM polymer film F7 (solid and dotted). The spectra reflect the average composition within the sampled region of the film independent of bond orientation effects due to the 'magic incidence angle' experimental geometry [3]. The P7 spectra recorded using the TEY (solid) and AEY (dotted) technique reflect the average composition of the outermost 10 nm and 1 nm from the film surface. The comparison reveals the enrichment of the surface with CF_3 groups. The peak assignment is in agreement with the literature [24–26].

The absorption spectra of the PFPM polymer film F7 as recorded by the AEY and TEY techniques are shown by the dotted and solid curves in Fig. 1, respectively. Comparing these to the PMMA spectrum, one finds again the absorption resonances associated with the C–H and C=O bonds. In addition, on top of the flat region in the PMMA absorption spectrum, pronounced absorption structures are observed that dominate the spectrum of the polymer F7. These peaks are related to excitations into the σ* orbitals of the $(CF_2)_n$ groups [24–26]. The peak just below 293 eV and the shoulder around 299 eV correspond to unoccupied C–F orbitals, the one in-between around 295 eV and a broad structure centered around 307 eV (clipped off in this figure) are related to the C–C bonds connecting the CF_2 groups of the side chains[2].

[2]The two weak bumps centered around 292.5 and 296 eV in the PMMA spectrum are the corresponding C–C resonances of the CH_2 groups in the PMMA backbone. The carbon atoms in the CF_2 groups have a positive charge in the ionic C–F bond, because of the high electronegativity of fluorine. In addition to localizing the electron orbitals, this also shifts the C–C excitations in the CF_2 groups to higher energies compared to the ones in the CH_2 groups.

A comparison of the two absorption yield spectra of F7 reveals in case of the AEY spectrum a decreased intensity of the C=O peak and an enhanced intensity in the 295–300 eV region. Since these spectra were recorded at a photon incidence angle of $\Theta = 54.7°$, the magic angle [3], they are free from bond orientation effects and simply represent the average chemical composition within the sampled subsurface regions. Hence, the comparison reveals that the top 1-nm surface region sampled by the AEY spectrum and the 10-nm subsurface region sampled in the TEY spectrum have different chemical compositions. A depletion of the carboxyl group concentration in the top surface region is indicated by the lower intensity of the C=O resonance in the AEY spectrum. The enhancement of the broad absorption structure between 295 and 300 eV, on the other hand, indicates an enrichment in the concentration of terminal CF_3 groups at the film surface. This conclusion is based on the fact, known from gas phase studies, that the spectral weight of the CF_3 group to the overall C K-edge absorption spectrum is shifted to higher energy relative to that of the CF_2 group [27]. This arises mainly from a chemical shift of the C 1s binding energy caused by the third fluorine atom bound to the terminal carbon atom [28]. Consequently, an enrichment of the surface region with CF_3 groups is reflected in an enhanced intensity in the spectral region between 295 eV and 300 eV.

The comparison of the AEY and TEY spectra thus verifies that CF_3 groups segregate to the film surface [5,8–10]. As these groups have a very low polarizability due to the strong ionic character of their chemical bonds, this enrichment of the surface with CF_3 groups explains the extremely low surface energies of these and related polymer films.

3.2. Preferential orientation

To understand the dependence of the NEXAFS spectra for linearly polarized X-rays on the relative orientation of the electric field vector and the molecular orientation at the polymer surface, imagine a single fluorocarbon chain oriented perpendicular to the surface. To a good approximation, this polymer chain will have all molecular C–F bonds oriented parallel to the surface. For a normal incidence geometry the electric field vector oscillates in the

surface plane. The dipole approximation then leads to maximum resonance intensities for all orbitals that are oriented parallel to the surface along the electric field vector. Hence, the C–F bond σ* resonance intensity would be largest. In a grazing incidence geometry, i.e. for a nearly perpendicular orientation of the electric field vector to the surface, all bonds oriented perpendicular to the surface would be emphasized. Those parallel to the surface, on the other hand, would be suppressed, and one would observe minimal intensity for the C–F bonds. Due to their near orthogonality C–F and C–C σ bonds are expected to show the opposite polarization dependence. In general, the transition probability, and hence the resonance intensity [29] depends on $\cos^2(\gamma)$, where γ is the angle between the electric field vector and the direction of the molecular orbital [3].

For a preferentially oriented ensemble of molecules with a uniaxial symmetry about the surface normal, the angular dependence of the absorption intensity is given by [17]

$$I(\Theta) = \alpha + \beta \cdot \sin^2(\Theta) \quad (1)$$

where Θ is the angle between the electric field vector of the incident photons and the surface normal. The parameters α and β measure the degree of orientation of the molecular bonds.

Fig. 2 shows the polarization dependence, or X-ray linear dichroism, of the AEY (left panel) and TEY (right panel) spectra of the three PFPM films at room temperature. The solid and dashed curves indicate spectra recorded at normal and grazing incidence, respectively. In these geometries the electric field vector is oriented parallel (solid) and nearly perpendicular (dashed) to the sample surface[3]. All spectra have in common that the C–F σ* resonances are stronger for the electric field vector oriented parallel to the film surface, while the C–C σ* resonances show the opposite polarization dependence, i.e. they are stronger for the electric field vector oriented perpendicular to the film surface. This indicates that within the sampled subsurface region the fluorocarbon side chains of all three polymers are preferentially oriented perpendicular to the film surface. Note that this is even the case for the polymer film F6, whose bulk has an isotropic distribution of side chain orientations.

Comparing the linear dichroism of the AEY (or TEY) spectra of the three films with each other, one notices that the polarization dependence increases with increasing length of the side chain, i.e. with increasing bulk order. This reveals that the order in the surface region follows that present in the bulk. Furthermore in each film the angular dependence of the AEY spectra is stronger than the one of the TEY spectra. Hence, in all three films the order in the surface region is larger than in the bulk.

The analysis of the sampling depth dependence of the NEXAFS signal in the previous section revealed that the lowering of the surface energy is due to an enrichment of the surface region in terminal CF_3 groups. Since this enrichment may be limited by the extent of side chain orientation, the surface energy appears to be lowered with increasing orientation of the fluorocarbon chains perpendicular to the film surface (CF_2 bonds parallel to the surface).

The presence of a preferential orientation of the C–F bonds revealed by the C K-edge linear dichroism implies that the F K-edge (1s) absorption spectrum should also show a polarization dependence. That this is indeed the case is demonstrated in Fig. 3, which compares F K-edge absorption spectra with the electric field vector oriented parallel (solid) and nearly perpendicular (dashed) to the film surface. A linear dichroism effect can clearly be observed for all three films, and its magnitude decreases as expected from F8, to F7 and F6, that is with decreasing degree of bulk order.

Since F atoms are solely located in the polymer side chains, the polarization dependence of the F K-edge absorption spectra is in principle better suited for the analysis of the preferential orientation of the side chains. However, due to the higher excitation energy, the F K-edge AEY spectrum is not as surface sensitive as the C K-edge AEY spectrum, rendering the differentiation between surface and bulk order less sensitive. Therefore only F K-edge TEY spectra are discussed.

[3]Due to the finite grazing incidence angle of 20 °C, the electric field vector is tilted 20° off the surface normal. Although this is not truly perpendicular to the film surface, we will refer to this simply as (nearly) perpendicular orientation.

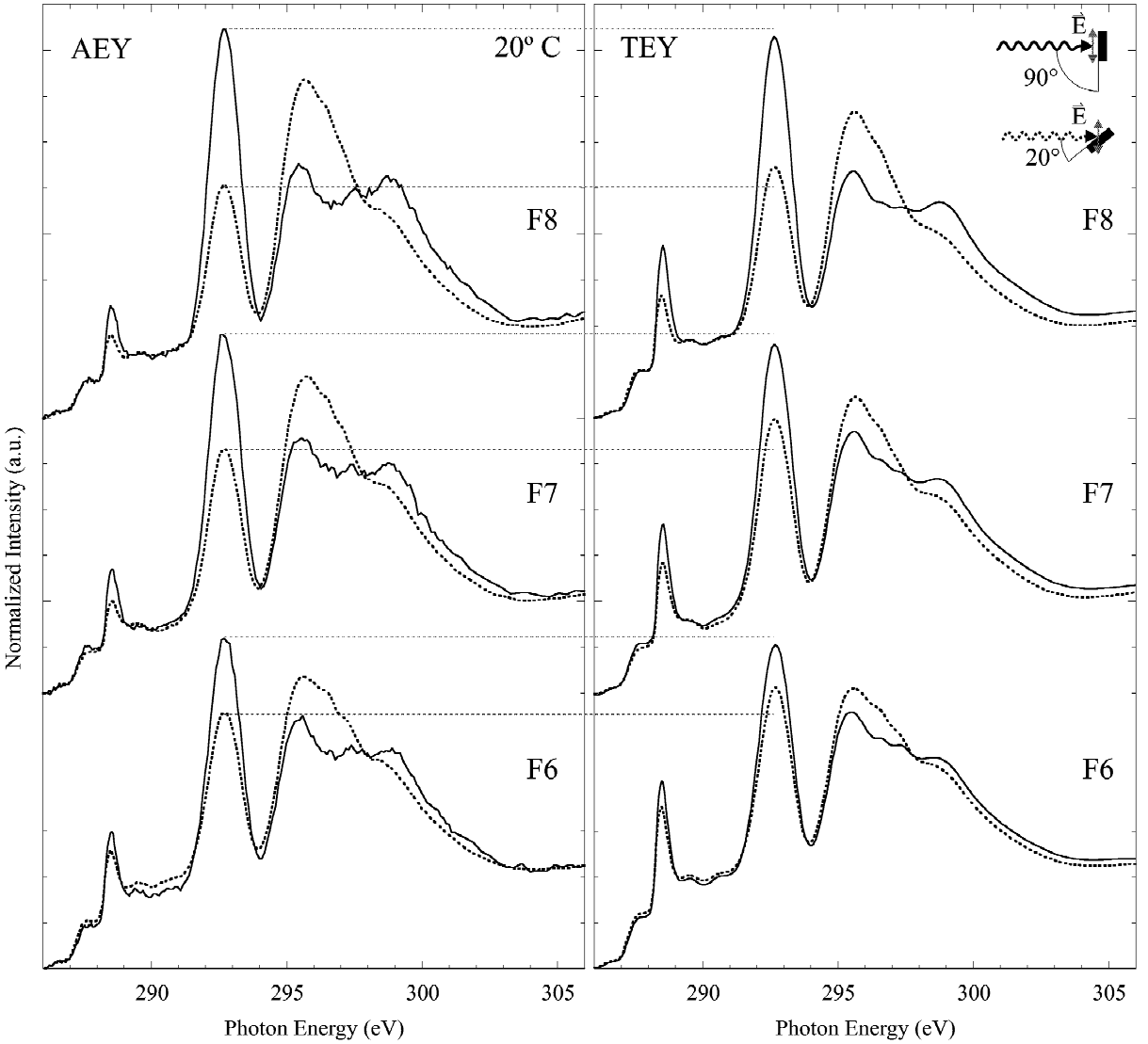

Fig. 2. Room temperature polarization dependence of the C K-edge NEXAFS spectra of the three PFPM polymer films. The linear dichroism shown by the AEY (left panel) and TEY (right panel) data reflects the degree of preferential orientation within the first 1 nm and 10 nm of the film surface, respectively.

3.3. Radiation damage

X-ray radiation damage is an important issue for polymer samples, in particular when it is already known that even exposure to UV or visible light damages a polymer. Since the sample damage scales with the accumulated dose of the incident radiation per area, we have reduced the incident photon flux density as discussed above. Our flux density of 7.5×10^{8} photons/(s·mm^{2}) was several orders of magnitude lower than what is typically used in synchrotron radiation experiments at 3rd generation synchrotron radiation sources, where on the order of 10^{11}–10^{12} photons/s are focused to spots of sub-millimeter dimensions.

The flux density of 7.5×10^{8} photons/(s·mm^{2})

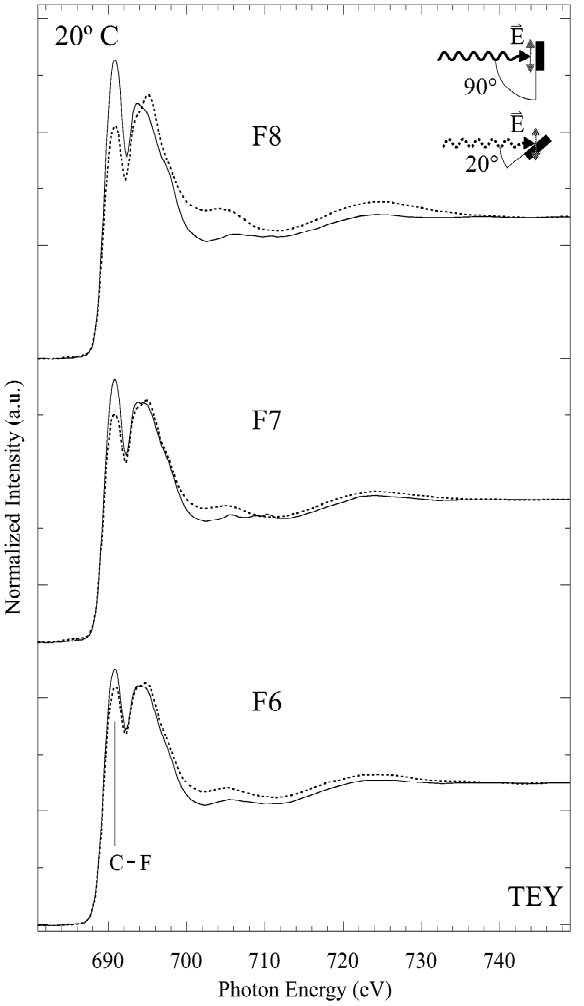

Fig. 3. TEY linear dichroism of the F K-edge (1s) NEXAFS spectra recorded at room temperature for the three PFPM polymer films. The first resonance is dominated by excitation into unoccupied σ*(C–F) states [25], while multiple absorption channels contribute to the other absorption structures.

was chosen as a compromise between acceptable signal-to-noise ratio in the spectra and suppression of sample damage. For the latter we used the criterion that the first and second spectrum recorded with the beam positioned on a fresh sample spot appeared identical. After longer exposure times, however, radiation damage effects were observable. Fig. 4A compares the initial C K-edge TEY spectrum recorded on a fresh spot (dotted) with the one recorded on that same spot after exposure to 5×10^{13} photons/

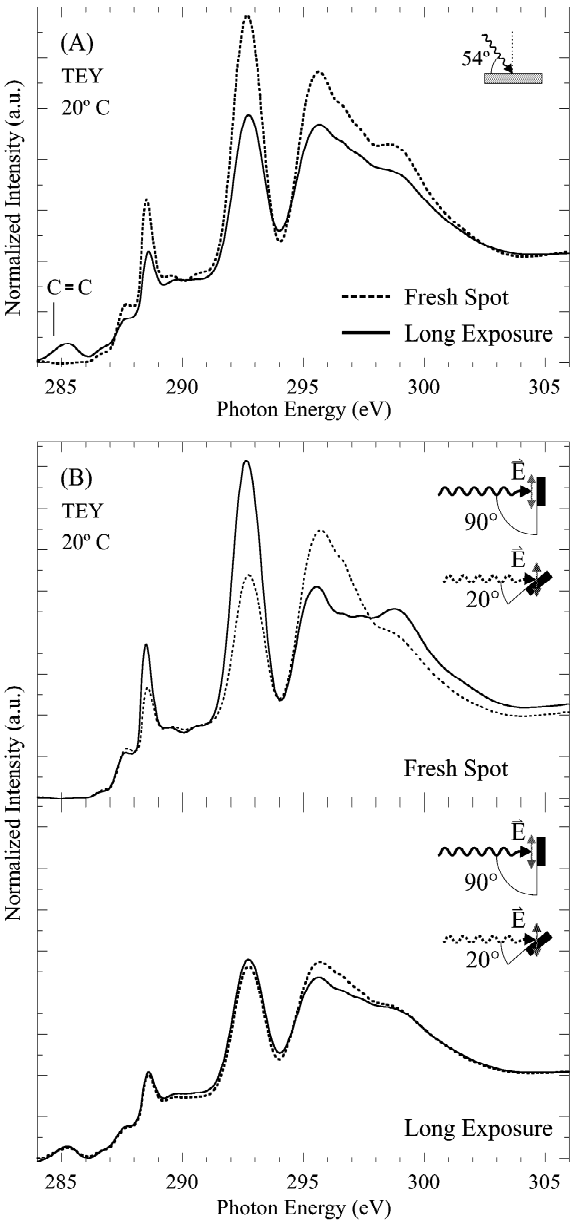

Fig. 4. Illustration of radiation damage of PFPM polymer films shown for the example of F8. (A) Chemical changes due to radiation damage as indicated by the comparison of the magic angle C K-edge NEXAFS spectra recorded on a 'fresh' spot (dotted) and after an exposure to 5×10^{13} photons/mm^2 (solid) of 300 eV. (B) Loss of preferential orientation due to radiation damage shown by the comparison of the linear dichroism measured for a fresh sample spot (upper panel) and a damaged spot after long exposure accumulating 5×10^{13} photons/mm^2 of 300 eV (lower panel).

mm^2 of 300 eV (solid), accumulated at a constant flux density of 7.5×10^8 photons/($s\cdot mm^2$). As the spectra were recorded in the magic angle geometry, the comparison reveals the average chemical composition changes within the sampled 10 nm subsurface layer. The strong reduction of the resonances associated with the CF_2 groups indicates that these groups have been broken apart, most likely with the fluorine atoms leaving the material. A reduction is also observed for the resonance related to the C=O bond of the carboxyl group and even for the preceding C–H peak. This loss of spectral weight in the resonances related to the PFPM polymer chains is accompanied by the appearance of a new peak around 285 eV, which is associated with unoccupied π^*-orbitals of C=C bonds. This indicates that the rupture of the polymer bonds leads to the formation of C=C double bonds, possibly within amorphous carbon like structures.

The chemical changes revealed by the comparison in Fig. 4A are accompanied by a strong loss of preferential orientation of the remaining fluorocarbon side chains, as shown in Fig. 4B. After radiation damage only a weak nearly negligible linear dichroism effect is found as shown in the lower panel of Fig. 4B. For comparison, the polarization dependence of the undamaged sample (fresh spot) is reproduced in the upper panel.

Despite the low flux density of 7.5×10^8 photons/($s\cdot mm^2$) one can observe first indications of radiation damage already after a few spectral scans. This is demonstrated in Fig. 5A by comparing the polarization dependence of the TEY spectra recorded on a fresh spot (left panel) to the one of the spectra recorded when repeating the absorption scan the tenth time (right panel), i.e. after an exposure to 5×10^{12} photons/mm^2 of around 300 eV. The overall decrease of the peak heights indicates that significant bond rupture has already occurred at this early stage of sample damage. Also, the preferential orientation appears to be reduced, which is indicated by the reduced magnitude of the observed linear dichroism effect[4].

A surprising observation is that in this early stage of sample damage we do not observe any chemical or orientation changes in the top surface region of about 1 nm, i.e. in the outermost 'layer' of fluorocarbon side chains. This is indicated by the AEY spectra, which have been recorded simultaneously with the TEY spectra of Fig. 5A. As shown in Fig. 5B, these AEY spectra (right panel) are identical, within experimental noise, to those of the initial scans (left panel). Since about the same number of photons is absorbed in the top 1 nm as in each of the deeper nm layers sampled in the TEY spectra, one would expect the degree of damage to be the same in the AEY and TEY data. This leads to the conclusion that some kind of bond healing must occur in the top surface layer. One may speculate that the atoms knocked out of the polymer chains in the deeper layers may be captured on their way out of the sample into the UHV environment of the experimental chamber by the broken bonds in the surface region. However, this conclusion is highly speculative and further experiments are required to understand the underlying process.

We note that this healing is only found in the initial stages of radiation damage. The AEY spectra recorded simultaneously with the TEY spectra of Fig. 4 (A) after exposure to 5×10^{13} photons/mm^2 of 300 eV, show comparable chemical changes and a similar reduction in preferential orientation as the TEY data.

3.4. Temperature dependence

The analysis of the room temperature data already indicates that although the order at the surface exceeds the one in the bulk, a well-ordered bulk nevertheless boosts the degree of surface order. The full importance of the bulk order, and in particular the link between bulk order and surface energy, follows from the temperature dependence of the linear dichroism as discussed below.

Fig. 6 shows the C K-edge TEY absorption spectra of the polymer films for three representative temperatures. Spectra recorded with the electric field vector aligned parallel and nearly perpendicular to the film surface are plotted as solid and dashed lines, respectively.

The left column of Fig. 6 shows TEY spectra recorded at 50 °C for the three samples. For each

[4]The order parameter calculated from the polarization dependence of the damaged spectra is reduced to about 90% of the one calculated for an undamaged spot.

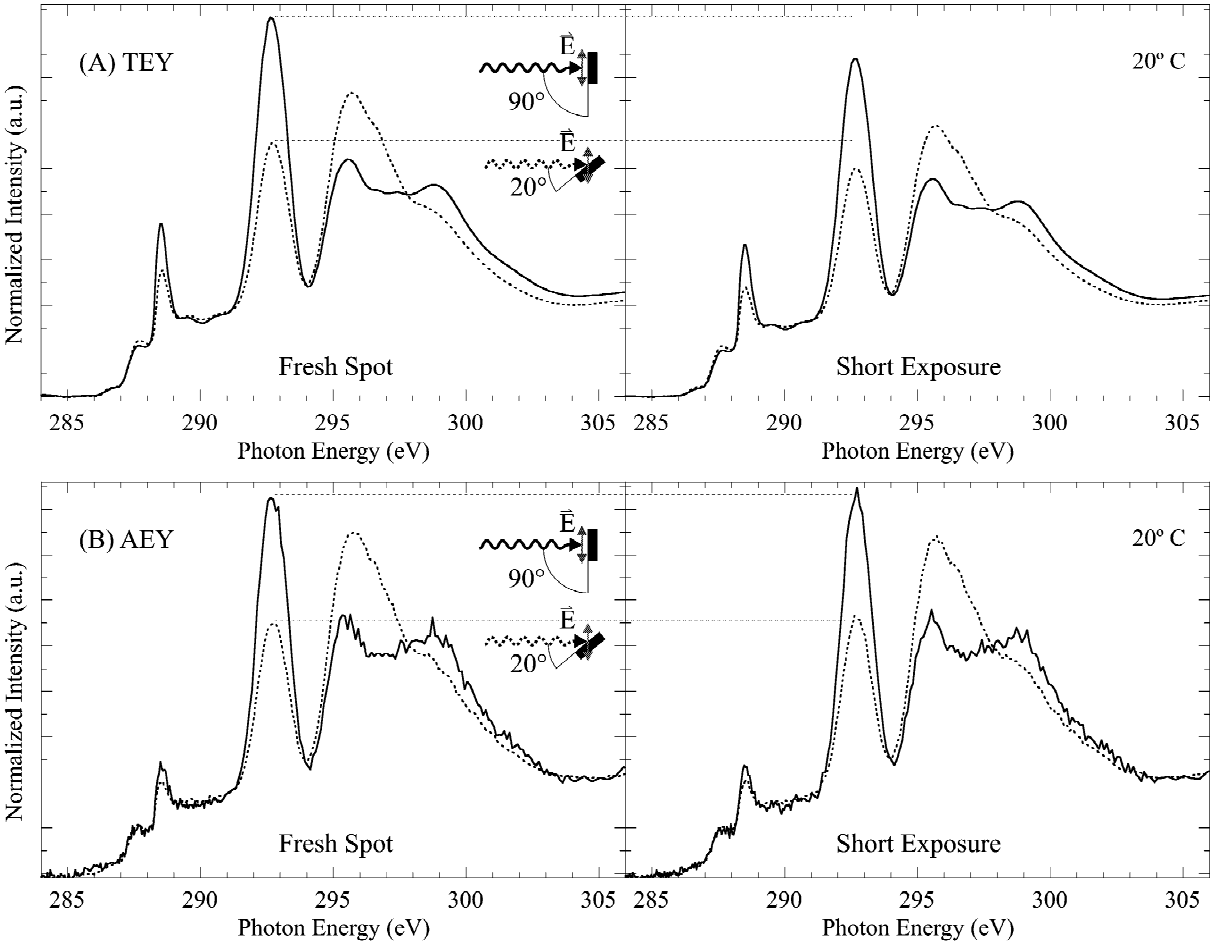

Fig. 5. Bulk versus surface radiation damage of PFPM polymer films shown for the example of F8: (A) Loss of preferential orientation in the early stages of radiation damage as given by the comparison of the polarization dependence of the more bulk sensitive TEY spectra recorded on a fresh spot (left panel) and after an accumulated exposure to 5×10^{12} photons/mm^2 (right panel) of 300 eV. (B) No radiation damage is revealed by the more surface sensitive AEY spectra recorded simultaneously with the TEY spectra shown in (A).

film the linear dichroism is slightly smaller than the one observed at 20 °C (Fig. 2). The relative differences between the three films, however, still resembles those found at room temperature. That is, the linear dichroism effect decreases with decreasing length of the side chains. Since at 50 °C the films have still the same bulk phases as at room temperature (smectic, nematic and isotropic), the strength of the linear dichroism decreases as before with decreasing structural order of the bulk phases. The slightly smaller amplitude of the linear dichroism effect at 50 °C compared to that at 20 °C, seen for each film, is attributed to increasing side chain fluctuation with temperature, which decreases the average preferential orientation.

For the polymer F6 a continuous decrease of the dichroism effect with temperature is indicated by the three sets of spectra in Fig. 6. At 140 °C, only a very faint linear dichroism is remaining, which shows that the film surface has become nearly as randomly

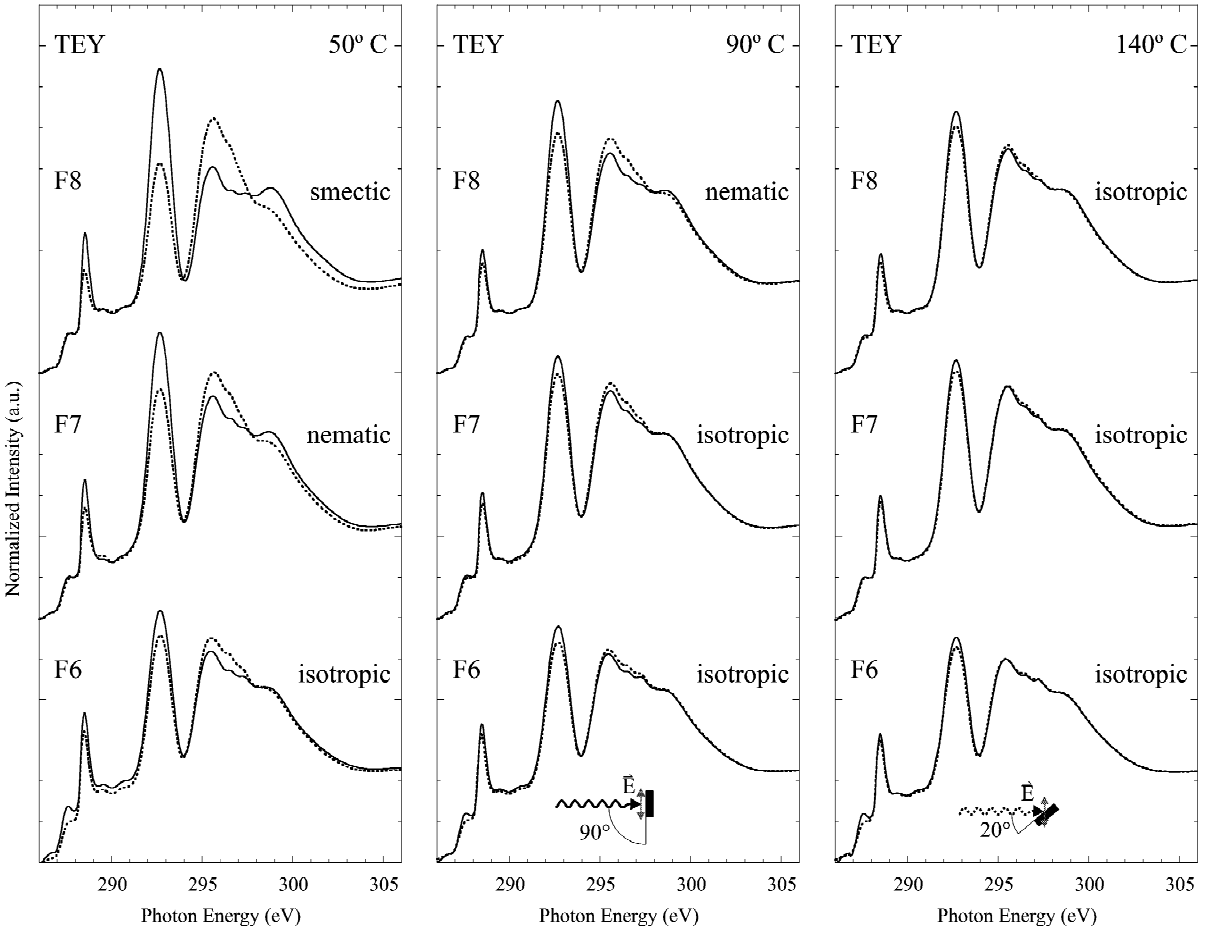

Fig. 6. Temperature dependence of the C K-edge polarization dependent NEXAFS spectra of the three PFPM polymers, recorded at 50 °C (left column), 90 °C, i.e. above the smectic to nematic (nematic to isotropic) bulk order phase transition of F8 (F7) (middle column), and 140 °C, where all three polymer films have an isotropic bulk order phase (right column). Note that for all studied temperatures the observed polarization dependence is independent of the annealing history of a particular film.

disordered as the bulk. The preferential orientation introduced by the presence of the film surface is nearly lost at this temperature.

Comparing the spectra of the polymer film F7 with the one of F6, one notices that for 90 and 140 °C the linear dichroism effect is virtually identical in the two films, while at lower temperatures it is significantly stronger for F7. This temperature dependence of their relative linear dichroism strength parallels the changes of their bulk structure. At 20 °C and 50 °C F7 has a more ordered bulk phase than F6, while they have the same isotropic, disordered bulk phase at 90 °C and 140 °C. A similar behavior is found for the temperature dependence of the linear dichroism of the polymer film F8, which changes its bulk phase from smectic to nematic to isotropic in the studied temperature range. At 90 °C F8 has a nematic bulk order and the observed linear dichroism exceeds the one of F7 and F6 with isotropic bulk order. At 140 °C F8 has an isotropic bulk phase and the magnitude of its dichroism is comparable to the one of F7 and F6. This strongly suggests that the

bulk order determines the achievable surface order, independently of the length of the PFPM side chains.

We note that the decrease of the linear dichroism with increasing temperature is completely reversible, i.e. when cooling the polymer films back to room temperature the initial dichroism effects are again observed.

3.5. Order parameter

For a quantitative analysis of the temperature dependence, it is beneficial to introduce an order parameter, S, which can be derived from the observed linear dichroism signal and constitutes a quantitative measure for the degree of preferential orientation [17]. Since the absorption measurement averages over all polymer side chains within the irradiated sample area, it is not possible to derive the microscopic orientation function of the side chains itself. One can, however, derive orientation factors f_i that describe the relative alignment along three orthogonal axes $i = (x, y, z)$, and hence describe any preferential orientation of the polymer side chain segments [30]. Due to the uniaxial symmetry about the surface normal z, i.e. the absence of any preferential orientation within the x–y film surface, one has the symmetry relationship

$$f_x = f_y = (1 - f_z)/2. \tag{2}$$

For purely linear polarized radiation and the electric field vector oriented parallel to the Cartesian axis $i = (x, y, z)$, the experimental absorption intensities I_i are given by

$$I_i = C \sum f_i \tag{3}$$

with $C = \Sigma_i I_i = I_{\text{tot}}$ for normalization of the factors f_i such that $\Sigma_i f_i = 1$. The connection to the experimentally observed polarization dependence as described by Eq. (1) is given by

$$f_z = \frac{A}{3A + 2B} \tag{4}$$

with $A = \alpha$ and $B = \beta$ for pure linear polarization. Otherwise, A and B can be calculated from the factors α and β taking into account the polarization degree of the X-rays [17].

It is common not to use f_z to describe the uniaxial distribution, but the order parameter S, which is defined as [30]

$$S = \frac{(3f_z - 1)}{2} = \frac{\left(\frac{3A}{3A + 2B} - 1\right)}{2}. \tag{5}$$

Hence, an ensemble that is perfectly aligned along the uniaxial symmetry axis has $S = 1$, while an isotropic distribution has $S = 0$. Negative values reflect a preferential orientation perpendicular to the symmetry axis with a maximum value of $S = -1/2$ indicating complete orientation within the plane perpendicular to the symmetry axis.

To quantify the degree of preferential orientation in the PFPM polymer films, we have used the polarization dependence of the single peak just below 293 eV, which is indicated by an arrow in Fig. 1. This peak is related to the excitation of C 1s core electrons into C–F σ^* orbitals of the CF_2 groups. Since the C–F orbitals are oriented perpendicular to the side chains, complete alignment of the side chains perpendicular to the film surface, i.e. parallel to the symmetry axis, corresponds to an order parameter of $S = -1/2$. From the angular dependence of the C–F resonance we can derive the parameters A and B, after subtracting the nearly flat background, indicated by the absorption spectrum of PMMA, on top of which the C–F absorption is located.

3.6. Bulk and surface order

The order parameters of the three films derived from the more bulk sensitive TEY data and the more surface sensitive AEY are summarized in Fig. 7. At room temperature the order parameters derived from the AEY data are $S = -0.16$ for F6, $S = -0.25$ for F7, and $S = -0.33$ for F8. Bearing in mind the room temperature surface energies of 10 dyn/cm for F6, 9 dyn/cm for F7, and 8 dyn/cm for F8, one notices that the surface energy correlates linearly with the order parameter derived from the more surface sensitive AEY data [31].

Comparing the two data sets in Fig. 7 one observes that for all temperatures the order parameter derived from the AEY data exceeds the corresponding one derived from the TEY data. Hence, the degree of preferential orientation is larger in the film

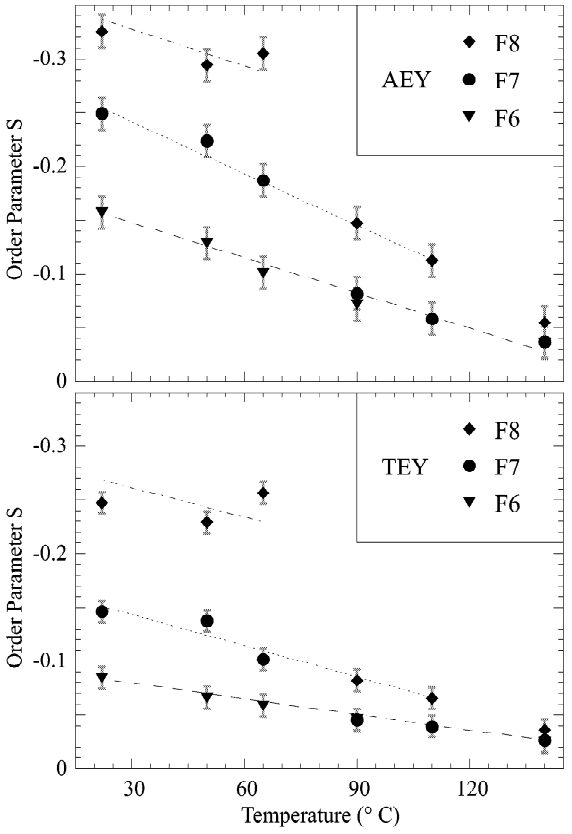

Fig. 7. Temperature dependence of the preferential orientation as quantified by the order parameter *S*, derived from the linear dichroism of the σ* (C–F) resonance around 293 eV in the C K-edge NEXAFS spectra. *S* describes the degree of order within the first 1 nm and 10 nm below the surface for the AEY and TEY data, respectively. The dotted line connects points corresponding to nematic bulk phases in F7 (below 80 °C) and F8 (above 80 °C), and the dashed line connects points corresponding to isotropic bulk phases in F6 (whole temperature range) and F7 (above 80 °C).

surface than in the film bulk over the whole temperature range.

Each set of order parameters, the AEY and the TEY data derived parameters, shows that with increasing temperature the degree of preferential orientation decreases. For each polymer, this decrease is continuous for the same bulk phase. Around the temperatures of bulk phase transitions, however, a step-like decrease in preferential orientation occurs. Furthermore, with increasing temperature, the difference between the degree of surface and bulk order decreases.

The most important observation, however, is that the quantitative order parameter analysis shows that the temperature dependent curves can be classified by the bulk order, independent of the side chain length. Each bulk phase has a characteristic (in first approximation) linear temperature dependence and data points from all three polymers follow these universal curves. For example, the dashed line in Fig. 7 represents the temperature dependence of the isotropic phase. It contains all data points for F6 which possesses an isotropic bulk phase over the entire temperature range. Above 80 °C the data points for F7, which assumes an isotropic bulk phase above about 80 °C, follow the dashed curve, too. The dotted line in Fig. 7 characterizes the temperature dependence of the nematic phase. It contains data points from both F7 and F8 films. In particular, one notices that above 80 °C the order parameter of F8 exhibits a drop of almost a factor of three, only to continue the extrapolated line from the lower temperature F7 nematic curve.

One obtains the same general trend shown in Fig. 7, if one derives the order parameter from the polarization dependence of the C–C resonance peak just below 296 eV. In this case, the background determination is complicated due to the close lying second C–F absorption structure, which has the opposite polarization dependence. Therefore, we shall not consider the results of this analysis here, but mention that the order parameters derived from the C–C and C–F data have the opposite sign due to the orthogonal orientation of these orbitals.

Furthermore, one can derive an order parameter from the polarization dependence of the F K-edge TEY absorption spectra shown in Fig. 3. One important difference to the C K-edge TEY spectra is that the TEY technique samples deeper below the surface for the F K absorption edge. This arises from the higher energy of the Auger electrons created in the decay of the F 1s core holes, which lead to a longer effective escape depth of the secondary electrons.

In Fig. 3 the first resonance around 690 eV is related to excitation of F 1s core electrons into the unoccupied σ*(C–F) orbitals of the CF_2 groups in the side chains [25]. Note that these are the same orbitals that are involved in the C 1s excitation associated with the resonance just below 293 eV (Fig.

2) whose dichroic intensity was used to derive the order parameter plotted in Fig. 7. Using the polarization dependence of this peak in the F K-edge absorption spectrum, one can calculate the order parameters summarized in Fig. 8. To do so we have estimated that the peak is located on a background due to other excitation channels, which has about 50% of the height of the F K-edge jump as defined by the absorption intensity high above the absorption edge around 750 eV. This estimate is based on the polarization dependence of well-ordered fluorocarbon chains studied by Ziegler et al. [25]. Note that an incorrectly estimated height of the background would affect all fluorine TEY derived order parameters in the same way. One can estimate, however, that this would alter the calculated order parameters by no more than 10%.

At first glance, Fig. 8 shows the same general behavior as Fig. 7. In particular, one finds again that the order parameter decreases continuously with temperature for a given bulk phase, independently of the particular polymer film. The order parameters derived from the fluorine TEY data, however, have smaller absolute values than the ones derived from the carbon TEY data. Since the TEY technique has at the F K-edge a larger sampling depth than at the C K absorption edge, this difference is in line with our previous observation that the more bulk sensitive C K-edge TEY data give smaller absolute values for the order parameter than the more surface sensitive C K-edge AEY data. Hence, going from the most bulk sensitive F K-edge data to the more surface sensitive C K-edge TEY and C K-edge AEY data, one obtains increasingly larger absolute values for the derived order parameters.

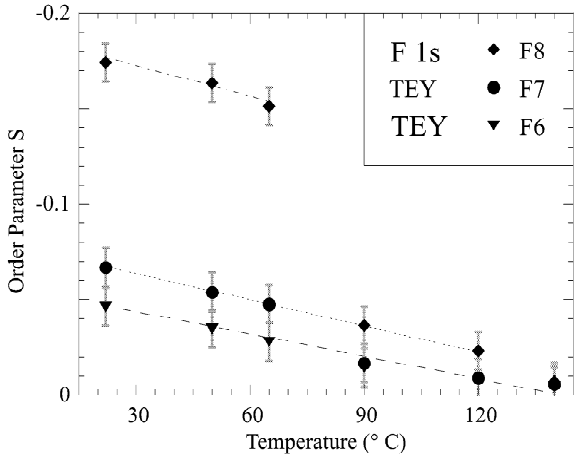

Fig. 8. Temperature dependence of the order parameter as derived from the polarization dependence of the σ*(C–F) resonance around 690 eV in the F K-edge TEY spectra shown in Fig. 3. These data show the same general behavior as found in Fig. 7, but the order parameters are significantly smaller than those derived from the C K-edge TEY data. As in Fig. 7, the dotted line connects points corresponding to nematic bulk phases in F7 (below 80 °C) and F8 (above 80 °C), and the dashed line connects points corresponding to isotropic bulk phases in F6 (whole temperature range) and F7 (above 80 °C).

Our combined results thus establish the importance of the bulk order for the surface energy of PFPM polymer films. Compared to other materials, the surface energy in all of these films is lowered by the segregation of CF_3 groups to the film surface, which inevitably results in an increase in the degree of preferential orientation in the surface region. The achievable preferential orientation in the surface region, however, is limited by the degree of preferential orientation present in the bulk of the film. In other words, the higher the degree of order in the bulk, the higher the surface order. The bulk order therefore limits the density and relative fraction of CF_3 groups in the surface region and thereby the lowering of the surface energy of the polymer films.

4. Conclusions

In summary, we have shown that the polarization dependence of the near edge X-ray absorption fine structure in the C and F K-edge absorption spectra offers a unique tool to investigate order phenomena in thin polymer films. The simultaneous acquisition of Auger and total electron yield spectra enabled us to separate surface and bulk contributions in the absorption spectra.

We applied this technique to investigate the origin of the low surface energy of thin perfluoroalkyl substituted polymethacrylates polymer films, which are currently used for a wide variety of applications. By studying the temperature dependence of bulk and surface order over a temperature range, which covers several bulk order phase transitions, we are able to unambiguously establish the role of the bulk order (phase). While the lowering of the surface energy is a

result of segregation of CF_3 groups to the film surface, it is the degree of bulk order, which ultimately limits the achievable surface energy lowering.

Acknowledgements

The authors thank K.Y. Song, C.J. Hawker, P. Iodice, and C.V. Nguyen from the IBM Almaden Research Center for help in sample preparation and characterization. Drs. S.Y. Park and J. Blackwell of the Case Western Reserve University, Cleveland, are acknowledged for carrying out the temperature dependent X-ray diffraction measurements which helped to determine the bulk order of the PFPM samples. DYY acknowledges the support of Brain Korea 21 Division of Chemistry and Molecular Engineering. This work was carried out in part at the Stanford Synchrotron Radiation Laboratory (SSRL), which is operated by the Department of Energy, Division of Chemical Sciences. The help of C. Troxel and J. Moore at SSRL is gratefully acknowledged.

References

[1] R.O. Ebewele, Polymer Science and Technology, CRC Press, Boca Raton, FL, 2000;
D. Dorel, Synthetic Polymers: Technology, Properties, Applications, Chapman and Hall, London, 1996.
[2] K. Siegbahn, ESCA Applied to Free Molecules, North Holland, Amsterdam, 1969.
[3] J. Stöhr, NEXAPS Spectroscopy, in: Springer Series in Sciences, Vol. 25, Springer, Heidelberg, 1992.
[4] G.E. Zaikov ((Ed.), Polymers in Medicine, Nova Science, New York, 1998;
E. Kissa, Fluorinated Surfactants, Synthesis–properties–applications, Marcel Dekker, New York, 1984.
[5] J. Wang, C.K. Ober, Macromolecules 30 (1997) 7560–7567.
[6] D.R. Iyengar, S.M. Perutz, C.-A. Dai, C.K. Ober, E.J. Kramer, Macromolecules 29 (1996) 1229.
[7] R. Defay, Surface Tension and Adsorption, Wiley, New York, 1966.
[8] J. Höpken, M. Möller, Macromolecules 25 (1992) 2482–2489.
[9] J. Wang, G. Mao, C.K. Ober, E.J. Kramer, Macromolecules 30 (1997) 1906–1914.
[10] D.L. Schmidt, C.E. Coburn, B.M. DeKoven, G.E. Potter, G.F. Meyers, D.A. Fischer, Nature 368 (1994) 39–41.
[11] L.D. Budovskaya, V.N. Ivanova, I.N. Oskar, S.V. Lukasov, Y.U.G. Baklagina, A.V. Sidorovich, D.M. Nasledov, Polymer Sci. USSR 32 (1990) 502–506.
[12] V.V. Volkov, N.A. Plate, A. Takahara, T. Kajiyama, N. Amaya, Y. Murata, Polymer 33 (1992) 1316–1320;
T. Shimizu, Y. Tanaka, S. Kutsumizu, S. Yano, Macromol. Symp. 82 (1994) 173–184;
T. Shimizu, Y. Tanaka, S. Kutsumizu, S. Yano, Macromolecules 29 (1996) 156–164;
V. Percec, M. Lee, J. Macromol. Sci. A 29 (1992) 723–740.
[13] P.G. De Gennes, J. Probst, The Physics of Liquid Crystals, Oxford University Press, New York, 1993.
[14] S. Sheiko, E. Lermann, M. Möller, Langmuir 12 (1996) 4015–4024.
[15] J.S. Wang, K. Matyjaszewski, J. Am. Chem. Soc. 117 (1995) 5614–5615;
J.S. Wang, K. Matyjaszewski, Macromolecules 28 (1995) 7901–7910.
[16] W.A. Zisman, Contact Angle, Wettability and Adhesion, American Chemical Society, Washington, DC, 1964.
[17] J. Stöhr, M.G. Samant, J. Electron Spectrosc. Relat. Phenom. 98 (1999) 189–207.
[18] M.O. Krause, J. Phys. Chem. Ref Data 8 (1979) 307.
[19] M.P. Seah, W.A. Dench, Surf. Interface Anal. 1 (1979) 2.
[20] M.G. Samant, J. Stahr, H.R. Brown, T.P. Russell, J.M. Sands, S.K. Kumar, Macromolecules 29 (1996) 8334–8342.
[21] S. Gota, M. GautierSoyer, M. Sacchi, Phys. Rev. B 62 (2000) 4187;
R. Nakajima, J. Stöhr, Y.U. Idzerda, Phys. Rev. B 59 (1999) 6421.
[22] L.G.M. Pettersson, H. Agren, B.L. Schurmann, A. Lippitz, W.E.S. Unger, Int. J. Quantum Chem. 63 (1997) 749.
[23] D.A. Outka, J. Stöhr, Chemistry and Physics of Solid Surfaces VII, 201, in: V.R. Vanselow, R. Howe (Eds.), Springer Ser. Surf Sci., Vol. 10, Springer, Berlin/Heidelberg, 1988.
[24] T. Ohta, K. Seki, T. Yokoyama, I. Morisada, K. Edamatsu, Phys. Script. 41 (1990) 150–153.
[25] Ch. Ziegler, Th. Schedel-Niedrig, G. Beamson, D.T. Clark, W.R. Salaneck, H. Sotobayashi, A.M. Bradshaw, Langmuir 10 (1994) 4399–4402.
[26] D.G. Castner, K.B. Lewis Jr., D.A. Fischer, B.D. Ratner, J.L. Gland, Langmuir 9 (1993) 537–542;
D.L. Schmidt, E.M. DeKoven, C.E. Coburn, G.E. Potter, G.F. Meyers, D.A. Fischer, Langmuir 12 (1996) 518–529.
[27] F.C. Brown, R.Z. Bachrach, A. Bianconi, Chem. Phys. Lett. 54 (1978) 425.
[28] M.B. Robin, I. Ishii, R. McLaren, A.P. Hitchcock, J. Electron Spectrosc. Relat. Phenom. 47 (1988) 53;
R. McLaren, S.A.C. Clark, I. Ishii, A.P. Hitchcock, Phys. Rev. A 36 (1987) 1683.
[29] J.J. Sakurai, Advanced Quantum Mechanics, Addison-Wesley, London, 1967.
[30] E.W. Thulstrup, J. Michl, Elementary Polarization Spectroscopy, VCH, New York, 1989.
[31] J. Lüning, J. Stöhr, K.Y. Song, C.J. Hawker, P. Iodice, C.V. Nguyen, D.Y. Yoon, Macromolecules 34 (2001) 1128.